A Joint Time and Frequency Synchronization and Channel Estimation for OFDM Systems Using One Training Symbol

Hlaing Minn and Vijay K. Bhargava

Department of Electrical and Computer Engineering, University of Victoria
Victoria, B.C., Canada V8W 3P6. Email: bhargava@ece.uvic.ca

Abstract – **A joint time and frequency synchronization and channel estimation for orthogonal frequency division multiplexing (OFDM) systems using only one training symbol is presented. The training symbol is composed of identical parts and the signs of these parts are designed in order to give a more pronounced timing metric trajectory peak. In order to avoid amplifier nonlinear distortion, the identical part is constructed based on the Golay complementary sequence. The proposed method utilizes the results of synchronization in the channel estimation stage and those of channel estimation in the synchronization stage, in an iterative way. The simulation results for a multipath Rayleigh fading environment show that the BER performance of the proposed method is very close to that of the ideal OFDM system with perfect synchronization and channel knowledge.**

Keywords: **OFDM, Timing synchronization, Frequency synchronization, Channel estimation, Training symbol**

I. Introduction

OFDM systems are much more sensitive to synchronization errors than single carrier systems [1] [2]. Several approaches have been proposed for time synchronization (e.g. [3]-[5]) and frequency synchronization (e.g. [6]-[10]), separately. All separate frequency synchronization methods assume perfect time synchronization, which may not be always guaranteed, and timing estimation errors may affect frequency synchronization performance. Hence, in order to evaluate actual performance, joint time and frequency synchronization approaches (e.g. [11]-[12]) are desirable. If coherent OFDM system is adopted, channel estimation becomes a necessity. Previous works on OFDM channel estimation (e.g. [13]-[15]) assume perfect synchronization, which may not be always guaranteed. As long as time synchronization gives the start of the OFDM symbol (useful part) in the inter-symbol interference (ISI) free interval, the time offset would not affect the channel estimation. However, frequency offset causes inter-subcarrier interference (ICI), which in turn deteriorates the channel estimation performance. Time offset may affect frequency synchronization and may therefore cause an indirect effect on the channel estimation performance. It would be more appropriate to evaluate the OFDM system performance by including synchronization and channel estimation.

Typically, one or two training symbols are used for time and frequency synchronization and another training symbol is used for channel estimation. In this paper, we present a joint time and frequency synchronization and channel estimation using only one training symbol. A specifically designed training symbol which gives a better coarse timing estimation is used. The timing synchronization performance is further improved by utilizing the channel estimation result. An approach to suppress the interference introduced to the frequency estimation is presented. The rest of the paper is organized as follows. Section II briefly describes the system considered and section III presents the proposed method. Performance evaluation by simulation is discussed in section IV and the conclusion is given in section V.

This work was supported in part by a Strategic Project Grant from the Natural Sciences and Engineering Research Council (NSERC) of Canada, and in part by Telus Mobility, Cellular.

II. System Description

The samples of a transmitted baseband OFDM signal, assuming ideal Nyquist pulse shaping, can be given by

$$s(k) = \frac{1}{\sqrt{N}} \sum_{n=0}^{N_u-1} c_n exp(j2\pi kn/N), \quad -N_g \le k \le N-1, \quad (1)$$

where c_n is the modulated data, N is the number of inverse Fast Fourier Transform (IFFT) points, $N_u (\le N)$ is the number of subcarriers, N_g is the number of guard samples and $j = \sqrt{-1}$. Consider a frequency selective multipath fading channel characterized by

$$h(k) = \sum_{l=0}^{K-1} h_l \delta(k - \tau_l) \quad (2)$$

where $\delta(k)$ represents the dirac-delta function, $\{h_l\}$ the complex path gains, $\{\tau_l\}$ the path time delays which are assumed in multiple of OFDM samples, and K the total number of paths. The received samples, if assuming perfect synchronization, are then given by

$$r(k) = \sum_{l=0}^{K-1} h_l s(k - \tau_l) + n(k) \quad (3)$$

where $n(k)$ is the sample of a zero mean complex Gaussian noise process with variance σ_n^2.

However, at the receiver, there exist carrier frequency offset, sampling clock errors and symbol timing offset which have to be estimated and compensated for. Usually frequency offset and timing error are more dominant than sampling clock inaccuracy and we will consider in this paper the carrier frequency and symbol timing synchronization assuming perfect sampling clock. The received samples then become

$$r(k) = exp(j2\pi kv/N) \sum_{l=0}^{K-1} h_l s(k - \tau_l - \varepsilon) + n(k) \quad (4)$$

where v is the carrier frequency offset normalized to subcarrier spacing and ε is timing offset in units of OFDM samples.

III. Proposed Joint Synchronization and Channel Estimation

In OFDM systems, the main synchronization parameters to be estimated are a sync flag indicating the presence of the signal (especially for burst mode transmission), the starting time of the FFT window (timing synchronization), the frequency offset between transmitter and receiver oscillators and the channel estimates if coherent reception is adopted.

The proposed scheme for joint synchronization and channel estimation of OFDM systems is shown in Fig. 1. A specifically designed training symbol is used. The sync flag is determined by the timing metric and threshold decision. In the following, we assume that the presence of the signal has already been detected and hence the rest of the synchronization part will be presented. First, coarse timing estimation is performed based on the timing metric. It gives the estimate of the start position of FFT window for the training symbol. Then frequency offset is estimated based on the training symbol defined by the coarse timing estimation. Then frequency offset compensation is performed on the training symbol. Next, channel impulse response is estimated based on the frequency offset compensated received training symbol. From channel estimation, the delay of the first channel path is found and added to the coarse timing estimate to give fine timing estimate. Then the new training symbol, defined by the fine timing estimate, is used to estimate fine frequency offset. Hence, the fine synchronization part contains frequency offset compensation, channel impulse response estimation, fine timing offset estimation, and fine frequency offset estimation. This fine synchronization can be repeated to achieve further improvement. The channel impulse response can then be estimated again after performing frequency offset compensation on the training symbol defined by fine timing estimate. Before transforming into the frequency domain, as a fine channel estimation stage, the channel impulse response estimate is further processed to suppress the noise.

III.1 Timing Metric

In *S&C* [12], a training symbol with two identical halves is used and the timing metric is given by

$$\mathcal{M}(d) = \frac{|P(d)|^2}{R^2(d)} \tag{5}$$

where $M = N/2$, d is the start of a window of N samples length and

$$P(d) = \sum_{i=0}^{M-1} r(i+d+M) \cdot r^*(i+d) \tag{6}$$

$$R(d) = \sum_{i=0}^{M-1} |r(i+d+M)|^2 \tag{7}$$

For the proposed scheme, the above timing metric, which is described for two identical parts, can be extended for the designed training symbol containing L parts of M samples each. Then, the constituents of (5) are given by:

$$P(d) = \sum_{k=0}^{L-2} b(k) \cdot \sum_{m=0}^{M-1} r^*(d+kM+m)\, r(d+(k+1)M+m) \tag{8}$$

$$R(d) = \sum_{m=0}^{N-M-1} |r(d+M+m)|^2 \tag{9}$$

and

$$b(k) = p(k)\, p(k+1), k = 0,\ 1,\ \ldots,\ L-2. \tag{10}$$

where $\{p(k) : k = 0,\ 1,\ \ldots,\ L-1\}$ are the signs of the identical parts which will be called the training symbol pattern in the rest.

III.2 Training Symbol

The training symbol of *S&C* gives a timing metric plateau which causes large timing estimator variance. This can be avoided by designing the training symbol to have a steep roll-off timing metric trajectory. Hence, we design the training symbol such that it is composed of L identical parts to handle frequency offset up to $\pm L/2$ subcarrier spacing and has a specific pattern (signs) of the L identical parts to give the timing metric with steep roll-off.

Suppose the training symbol (excluding cyclic prefix) is composed of L identical parts as $[\pm A,\ \pm A,\ \ldots,\ \pm A]$ where A represents the basis part. Then if the timing metric given in (5)(8)(9) is used, the best training symbol patterns obtained by computer search are given in Table I for 10% cyclic prefix and $L = 4$, 8 and 16. These patterns are obtained by finding the patterns that give the minimum value of the sum of the correlation metric (i.e., the area of the correlation metric trajectory) over about a two-symbol interval with correct timing at the middle. These generally produce the steepest roll-off timing metric from the correct timing point. The sign inversion of the patterns shown in Table I can also be used. The trajectories of timing metrics used in coarse timing estimation for the training symbol patterns (the first one for each L case), given in Table I, are shown in Fig. 2 under no channel distortion and no noise condition. The timing metric trajectory of *S&C* is also included for comparison. Unlike *S&C*, there is no timing metric trajectory plateau associated with the proposed method. The larger value of L gives the timing metric trajectory with the steeper roll-off.

In order to avoid nonlinear distortion at the transmitter, the training symbol should be designed to have a low peak-to-average power ratio (PAPR). Golay complementary sequences [20] are well known for having good correlation properties which translate into very a low PAPR value ($3\,dB$) when they are used to modulate as an OFDM signal [21]. In our training symbol design, the basis part has $M = N/L$ samples (for N point IFFT and L identical parts) and is generated by M point IFFT of length N_u/L Golay complementary sequence.

III.3 Coarse Timing Estimation

Coarse timing estimation is based on the correlation among L parts of size M samples each. The coarse timing estimator chooses as the start of OFDM

symbol (after cyclic prefix) the maximum point, d_{max}, of the timing metric given by (5)(8)(9). In order to restore orthogonality among subcarriers, the timing estimate should be in the ISI free part of the cyclic prefix. In AWGN channel, the mean of the proposed timing metric trajectory peak is at the exact timing point, whereas in multipath channels, it would be shifted (delayed) due to the channel dispersion. Hence the coarse timing estimate $\hat{\varepsilon}_c$ should be pre-advanced by some samples λ_c as

$$\hat{\varepsilon}_c = d_{max} - \lambda_c \tag{11}$$

where λ_c should be chosen larger than the (designed) mean shift of the timing point caused by the channel dispersion.

III.4 Carrier Frequency Offset Estimation

For carrier frequency estimation, we follow the method of $M\&M$ [10] with appropriate modification. Since the only difference in the training symbol structure is the sign pattern of L identical parts, the training symbol defined by timing estimator is first modified to have the same structure as $M\&M$ by multiplying the L parts with the sign pattern applied in the training symbol design. Then the method of $M\&M$ is applied with $H = L/2$ in Eq.(13) of [10]. The frequency offset estimation range is $\pm L/2$ subcarrier spacing for the training symbol with L identical parts. However, the range is not limited by the length of sign pattern (L) in our design. For example, by designing the basis part to have k identical subparts, the range becomes $\pm L\ k/2$.

However, in multipath dispersive channel, the basis parts of the received training symbol will not be equal, even in the absence of noise, due to the sign conversion in the transmitted training symbol. This effect deteriorates the repetitive nature of the received training symbol. For frequency estimation, the received training symbol is multiplied with the sign pattern to restore the repetitive parts. But this sign flipping will not remedy the already deteriorated repetitive parts. Hence, some interference is introduced to frequency estimation. To suppress this interference, the differently affected received samples can be excluded from the frequency estimation. For $L = 4$ case, by excluding the first τ_{max} samples (designed maximum channel delay spread) of the second and the third basis parts, the interference can be suppressed. The exclusion of those samples can easily be done by masking them with zeros. Then the modified procedure becomes zero masking, sign flipping and applying $M\&M$. This zero masking approach can be applied if the number of samples in the basis part is much larger than the maximum channel delay spread.

III.5 Channel Estimation

Assume that the channel response remains constant over at least one OFDM symbol interval (quasi-static case) and let the instantaneous path gains be $h_0, h_1, \ldots, \ldots, h_{K-1}$. Let us define the following:

$$\begin{aligned}
\mathbf{r}(0) &\triangleq [r(0)\ r(1)\ \ldots\ r(N-1)]^T \\
\mathbf{h} &\triangleq [h(0)\ h(1)\ \ldots\ h(K-1)]^T \\
\mathbf{W}(v) &\triangleq diag\{0,\ e^{j2\pi v/N},\ e^{j2\pi 2v/N},\ \ldots,\ e^{j2\pi(N-1)v/N}\} \\
\mathbf{n} &\triangleq [n(0)\ n(1)\ \ldots\ n(N-1)] \\
\mathbf{S} &\triangleq \begin{bmatrix} s(0) & s(-1) & \ldots & s(-K+1) \\ s(1) & s(0) & \ldots & s(-K+2) \\ & \ddots & & \\ s(N-1) & s(N-2) & \ldots & s(N-K) \end{bmatrix}
\end{aligned} \tag{12}$$

where $\{s(k) : k = 0, 1, \ldots, N-1\}$ are the samples of the transmitted training symbol, $\{r(k) : k = 0, 1, \ldots, N-1\}$ the corresponding received samples, $\{n(k) : k = 0, 1, \ldots, N-1\}$ the noise samples and v the normalized frequency offset.

Then the received samples vector can be given by

$$\mathbf{r}(0) = \mathbf{W}(v) \cdot \mathbf{S} \cdot \mathbf{h} + \mathbf{n} \tag{13}$$

The channel response estimate can be obtained by [18]

$$\hat{\mathbf{h}} = [\mathbf{S}^H \cdot \mathbf{S}]^{-1} \mathbf{S}^H \cdot \mathbf{W}^H(\hat{v}) \cdot \mathbf{r}(0) \tag{14}$$

In the above channel estimation, the maximum channel delay spread is required. Moreover, due to the timing estimation error and pre-advancement of the timing estimate, the received training vector will be $\mathbf{r}(\varepsilon)$. The pre-advancement of the timing offset estimate should be such that ε is negative most of the time; otherwise it will not only introduce ISI but also miss some channel taps in the channel estimation and cause some channel estimation error. Consequently, the designed maximum channel delay spread should also be longer than the actual maximum channel delay spread plus the delay introduced by timing estimate pre-advancement. Let the designed maximum channel delay spread be K'. By replacing K with K' in (12), the channel response estimate is given by

$$\hat{\mathbf{h}} = [\mathbf{S}^H \cdot \mathbf{S}]^{-1} \mathbf{S}^H \cdot \mathbf{W}^H(\hat{v}) \cdot \mathbf{r}(\varepsilon) \tag{15}$$

where $\mathbf{W}^H(\hat{v}) \cdot \mathbf{r}(\varepsilon)$ is the frequency offset compensated received training vector defined by timing estimate ε.

III.6 Fine Timing and Frequency Offset Estimation

The coarse timing estimate would be, most of the time, before the actual timing point due to the pre-advancement. However, even under no noise condition, the timing estimate would be varying according to the time-varying nature of the channel response. Accordingly, at different snap-shots, the channel estimates would be delayed by different amounts due to different timing offset errors. If the delay in the channel estimate can be found, the effect of the time-varying channel response on the timing estimation can be removed by simply delaying the coarse timing estimate by the same amount of the channel estimate delay. In other words, the coarse timing estimate can be fine-tuned by adding the delay of the first actual channel tap from the channel estimate.

One way of finding the delay of the first actual channel tap is described in the following. First, the strongest tap gain, h_{max}, is found and then the first actual channel tap is estimated as the first estimated channel tap whose absolute tap gain is greater than $\alpha \cdot |h_{max}|$. Mathematically, $h_{max} = max\{h_i :\ i = 0,\ 1,\ \ldots,\ K'-1\}$ and the delay of the first actual channel tap τ_0 is given by

$$\tau_0 = min\{i :\ |h_i| > \alpha \cdot |h_{max}|\} \tag{16}$$

The choice of α may depend on the channel power delay profile, especially the ratio of the absolute gains of the first and the strongest taps. In order to avoid missing the first tap, α should be much smaller than this ratio. On the other hand, α should not be too small; otherwise noise will increase the probability of wrongly picking up the channel tap before the first tap. In this sense, the choice of α also depends on the channel estimation noise.

The fine timing estimate is obtained by adding the delay of the first actual channel tap to the coarse timing estimate as

$$\hat{\varepsilon} = \hat{\varepsilon}_c + \tau_0 - \lambda_f \tag{17}$$

where λ_f is a designed pre-advancement to reduce the possible ISI.

On the other hand, the pre-advancement of fine timing estimate may introduce interference in frequency offset estimation. Hence, a better choice of the received training symbol for frequency offset estimation should be defined by the fine timing estimate without pre-advancement and the fine timing estimate is then advanced by λ_f as in (17). In this way, the timing offset error interference in frequency offset estimation can be reduced and at the same time, the ISI caused by the timing offset error can be reduced by means of pre-advancement.

For a multipath channel with an exponential power delay profile, simply using the strongest channel tap's delay instead of the first tap's delay would achieve a similar performance.

III.7 Fine Channel Estimation

For a WSSUS multipath channel, if the channel statistics and SNR are known *a priori*, the linear minimum mean square error (LMMSE) estimator can be implemented as follows:

$$\hat{\mathbf{h}}_{mmse} = diag\{\frac{\sigma_{h_0}^2}{\sigma_{h_0}^2 + 1/SNR}, \frac{\sigma_{h_1}^2}{\sigma_{h_1}^2 + 1/SNR}, \cdots, \frac{\sigma_{h_{N-1}}^2}{\sigma_{h_{N-1}}^2 + 1/SNR}\} \hat{\mathbf{h}}_{LS} \tag{18}$$

where $diag\{a_0,\ a_1,\ \ldots,\ a_{N-1}\}$ is a diagonal matrix with diagonal elements $[a_0,\ a_1,\ \ldots,\ a_{N-1}]$ and $\sigma_{h_i}^2$ is the power contained in the i^{th} channel path.

However, since multipath channel statistics and SNR are usually unknown at the receiver, some fixed values have to be used for them. In [16], it is suggested to use a high dummy SNR value and a uniform multipath channel correlation, which are robust to the channel correlation mismatch. From (18), with a high dummy SNR value, the LMMSE approach can be viewed as setting the channel taps with no energy to zeros and bypassing other taps.

Since most practical multipath channels have only a few significant paths, a suitable way of implementing an approximate LMMSE is by choosing a predefined number of the most significant taps and setting the others to zero (e.g., [19]). This approach is adopted in our scheme.

IV. Simulation Results and Discussions

IV.1 Simulation Parameters

The performance of the proposed synchronization algorithm has been investigated using computer simulation. The OFDM system parameters used are 1024 subcarriers, 1024 point $IFFT/FFT$, 10% guard interval (102 samples), a carrier frequency offset of 6.2 subcarrier spacing, QPSK data modulation and 10,000 simulation runs. The training symbol pattern for $L = 4$ is used. The other parameters used are: $(\lambda_c = 20)$ in the coarse timing estimation, $K' = 84$ in the channel estimation and $\alpha = 1/5,\ \lambda_f = 20$ for fine timing estimation. The timing estimator performance of $S\&C$ with 90% point averaging is included for comparison. Multipath Rayleigh fading channel is assumed to have an exponential power delay profile. The number of channel taps is 16 and equal channel tap spacings of 4 samples are used. The ratio of the first tap to the last tap is set to $20dB$. The channel estimation and BER performances are evaluated using 1,000 simulation runs with one training and 10 data symbols in each run. In fine channel estimation, the number of most significant taps used is 16.

IV.2 Results and Discussions

The missed detection and false detection probabilities of the proposed scheme and $S\&C$ in the multipath Rayleigh fading channel described above are shown in Fig. 3. For the proposed scheme, the same timing metric of the coarse timing estimation is used for the detection of the sync flag. The false detection probabilities are evaluated in the presence of data signal (not training signal). Also shown are the false detection probabilities when only noise is present. From Fig. 3, it is observed that both methods provide very robust synchronization. For the same missed detection probability, the timing metric threshold of $S\&C$ has a higher value than the proposed method, but the same holds for the false detection probability. Hence, both methods can be considered as having similar sync detection capability.

Table II shows the mean and the variance of the timing estimation observed in the simulation. Also shown are the average interference-to-signal ratio $1/SIR_\varepsilon$ caused by timing estimation errors. The interference-to-signal ratio $1/SIR(\varepsilon)$ for each timing offset ε is given by

$$\frac{1}{SIR(\varepsilon)} = \frac{\sigma_\varepsilon^2}{\alpha^2(\varepsilon)} \tag{19}$$

Due to space limitation, the expression for $\alpha(\varepsilon)$ and σ_ε^2 are referred to [17]. The better performance of the proposed method can easily be observed from the results. The zero interference-to-signal ratio of the proposed method means that in the simulation the timing estimates are always in the ISI-free interval.

Table III shows the frequency estimation performance of the proposed scheme in terms of the frequency estimation variance and the average interference-to-signal ratio $1/SIR_v$ caused by the frequency estimation errors. The performance of $M\&M$ [10] with perfect timing is also included as a reference. The interference-to-signal ratio caused by a normal-

ized frequency estimate error Δ_v is obtained by [17]:

$$\frac{1}{SIR_v(\Delta_v)} \simeq \frac{\pi^2}{3} \cdot {\Delta_v}^2 \tag{20}$$

From the results, it can be observed that the frequency estimation performance of the proposed method is very close to that of $M\&M$ with perfect timing.

Fig. 4 shows the channel estimation mean square error (MSE) of the proposed method without assuming the perfect timing and frequency synchronization. The MSE of the least square method (LS), which is equal to $1/SNR$, is also included as a base reference. The performance gain of the proposed method over LS is a result of noise suppression in the channel estimation. It should be mentioned that the channel estimation performance shown is optimistic due to two conditions: the channel taps are sample-spaced and the number of the most significant taps used in the channel estimation is exactly the same as the number of channel tap. For a channel with non-sample spaced taps, a larger number of most significant taps should be used to account for the channel energy leakage and a slight performance degradation can be expected.

Fig. 5 shows the BER performance of the proposed method in the multipath Rayleigh fading channel. Also shown is the BER performance of the ideal system with perfect timing and frequency synchronization and perfect channel estimation. At low SNR region, the proposed method has just about 1 dB SNR degradation from the ideal case and at high SNR region the proposed method's performance is very close to the ideal case's performance. The BER performance loss of the proposed method is due to the nonperfect synchronization and channel estimation. As SNR increases, the synchronization and channel estimation performances get improved and hence the proposed method's BER performance becomes very close to the ideal case's.

V. Conclusion

A robust time and frequency synchronization and channel estimation using one training symbol is presented. The training symbol is designed in such a way that the amplifier nonlinear distortion is avoided and a better coarse timing estimation accuracy is achieved. In the proposed method, the results of the synchronization is utilized in the channel estimation, and vice versa. The computer simulation results for a multipath Rayleigh fading environment show that while reducing the overhead by using one training symbol, the proposed method also achieves a BER performance very close to the ideal case with perfect synchronization and perfect channel estimation.

VI. References

[1] T. Pollet, M. Van Bladel and M. Moeneclaey, "BER sensitivity of OFDM systems to carrier frequency offset and wiener phase noise," *IEEE Trans. on Comms.*, Vol. 43, No. 2/3/4, Feb/Mar/Apr 1995, pp. 191-193.

[2] M. Gudmundson and P.O. Anderson, "Adjacent channel interference in an OFDM system," *Proc. Vehicular Tech. Conf*, Atlanta, GA, May 1996, pp. 918-922.

[3] M. Speth, F. Classen and H. Meyr, "Frame synchronization of OFDM systems in frequency selective fading channels," *Proc. Vehicular Tech. Conf.*, Phoenix, Arizona, USA, May 1997, pp. 1807-1811.

[4] M. Speth, D. Daecke and H. Meyr, "Minimum overhead burst synchronization for OFDM based broadband transmission," *Proc. Global Telecom. Conf.*, Sydney, Australia, Nov 1998, pp. 2777-2782.

[5] D. Landström, S.K. Wilson, J.J. van de Beek, P. Ödling and P.O. Börjesson, "Symbol time offset estimation in coherent OFDM systems," *Proc. Intl Conf. on Communications*, Vancouver, BC, Canada, June 1999, pp. 500-505.

[6] P.H. Moose, "A technique for orthogonal frequency division multiplexing frequency offset correction," *IEEE Trans. on Comms.*, Vol. 42, No. 10, Oct 1994, pp. 2908-2914.

[7] F. Classen and H. Meyr, "Frequency synchronization algorithms for OFDM systems suitable for communication over frequency selective fading channels," *Proc. Vehicular Tech. Conf*, Stockholm, Sweden, Jun 1994, pp. 1655-1659.

[8] F. Daffara and O. Adami, "A new frequency detector for orthogonal multicarrier transmission techniques," *Proc. Vehicular Tech. Conf*, Chicago, Illinois, USA, Jul 1995, pp. 804-809.

[9] H. Nogami and T. Nagashima, "A Frequency and Timing Period Acquisition Technique for OFDM Systems," *IEICE Trans. Comms.*, Vol. E79-B, No. 8, Aug 1996, pp. 1135-1146.

[10] M. Morelli and U. Mengali, "An improved frequency offset estimator for OFDM applications," *IEEE Comms. Letters*, Vol. 3, No. 3, Mar 1999, pp. 75-77.

[11] J-J. van de Beek, M. Sandell and P.O. Börjesson, "ML estimation of time and frequency offset in OFDM systems" *IEEE Trans. Signal Proc.*, Vol. 45, no. 7, July 1997, pp. 1800-1805.

[12] T. M. Schmidl and D. C. Cox, "Robust Frequency and Timing Synchronization for OFDM," *IEEE Trans. on Comms.*, Vol. 45, No. 12, Dec 1997, pp. 1613-1621.

[13] J.-J. van de Beek, O. Edfors, M. Sandell, S. K. Wilson and P. O. Borjesson, "On channel estimation in OFDM systems," *IEEE Vehicular Technology Conf.*, Chicago, IL, July 1995, pp. 815-819.

[14] O. Edfors, M. Sandell, J.-J. van de Beek, S. K. Wilson and P. O. Borjesson, "OFDM channel estimation by singular value decomposition," *IEEE Trans. on Commun.* vol. 46, Jul 1998, pp. 931-939.

[15] Y. Li, L. J. Cimini, Jr., and N. R. Sollenberger, "Robust channel estimation for OFDM systems with rapid dispersive fading channels," *IEEE Trans. on Commun.*, vol. 46, Jul 1998, pp.902-915.

[16] O. Edfors, M. Sandell, J. -J. van de Beek, S. K. Wilson and P. O. Brjesson, "OFDM channel estimation by singular value decomposition," *IEEE Trans. Commun.*, Vol. 46, July 1998, pp. 931-939.

[17] M. Speth, S. A. Fechtel, G. Fock and H. Meyr, "Optimum receiver design for wireless broad-band systems using OFDM-Part I," *IEEE Trans. Commun.*, Vol. 47, No. 11, Nov. 1999, pp. 1668-1677.

[18] S. A. Fechtel and H. Meyr, "Fast frame synchronization, frequency offset estimation and channel acquisition for spontaneous transmission over unknown frequency-selective radio channels," *PIMRC*, Yokohama, Japan, 1993, pp. 229-233.

[19] Y. Li, L. J. Cimini, Jr., and N. R. Sollenberger, "Robust channel estimation for OFDM systems with rapid dispersive fading channels," *IEEE Trans. on Commun.*, vol. 46, pp. 902-915, Jul 1998.

[20] M.J.E. Golay, "Complementary series," *IRE Trans. on Information Theory*, Vol. IT-7, Apr 1961, pp. 82-87.

[21] R.D.J. van Nee, "OFDM codes for peak-to-average power reduction and error correction," *Proc. Global Telecom. Conf.*, London, Nov 1996, pp. 740-744.

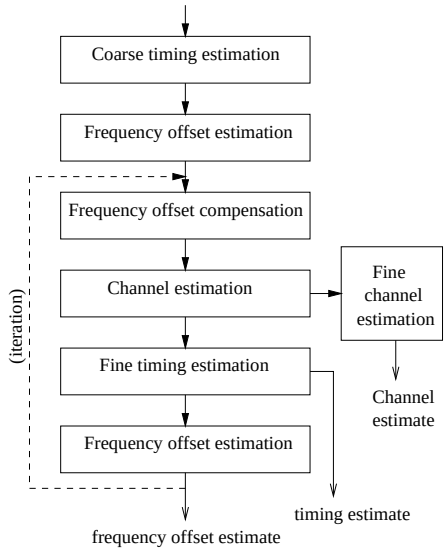

Fig. 1. Proposed joint synchronization and channel estimation

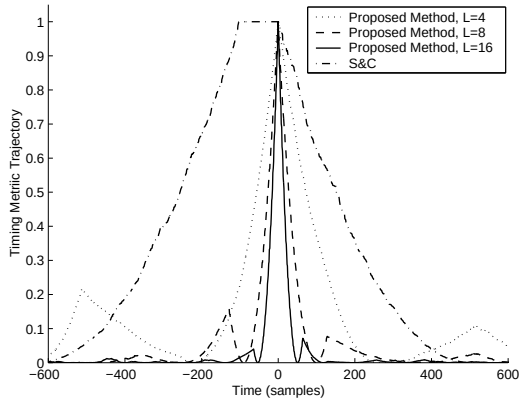

Fig. 2. Timing metric under no channel distortion and noise condition. (Time index 0 corresponds to exact timing point.)

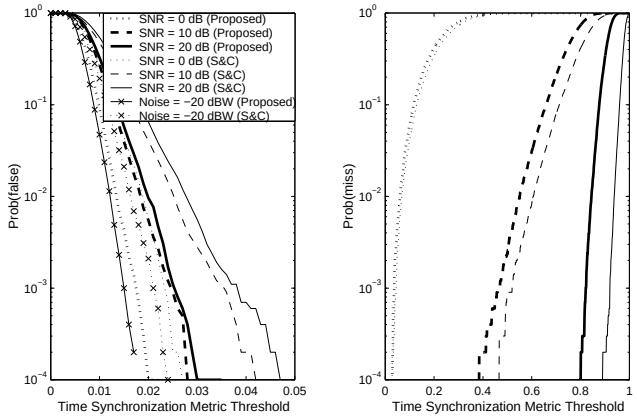

Fig. 3. Sync Detection Performance in the multipath Rayleigh fading channel

TABLE I
TRAINING SYMBOL PATTERN

L	$Pattern$
4	$(-+--)$
	$(++\,+-)$
8	$(++--+---)$
	$(-++---+-)$
16	$(+--++--+-++-+--)$
	$(--+-+-+---+++-)$

TABLE II
TIMING ESTIMATION PERFORMANCE

Method	SNR (dB)	Mean (sample)	Variance (sample^2)	$1/SIR_\varepsilon$
$S\&C$	0	-39.11	467.85	1.4×10^{-3}
	10	-39.50	43.92	1.44×10^{-5}
	20	-39.42	36.60	1.07×10^{-5}
Proposed	0	-19.94	17.86	4.60×10^{-5}
	10	-19.55	2.53	0
	20	-19.59	2.22	0

TABLE III
FREQUENCY ESTIMATION PERFORMANCE

Method	SNR (dB)	Variance	$1/SIR_v(dB)$
$M\&M$	0	2.33×10^{-4}	-31.15
(perfect timing)	10	1.77×10^{-5}	-42.36
	20	1.79×10^{-6}	-52.31
Proposed	0	2.66×10^{-4}	-30.58
(zero masking)	10	1.94×10^{-5}	-41.95
	20	1.89×10^{-6}	-52.05

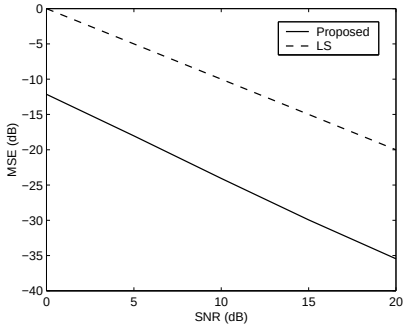

Fig. 4. Channel estimation performance in the multipath Rayleigh fading channel

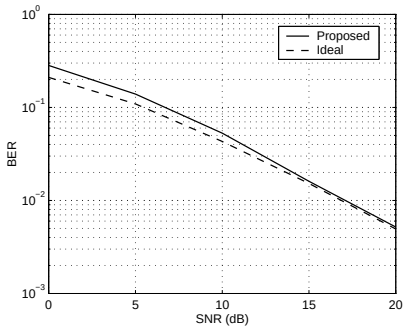

Fig. 5. BER performance in the multipath Rayleigh fading channel.